Archives of Hydro-Engineering and Environmental Mechanics
Vol. 52 (2005), No. 3, pp. 213–242

Theoretical Analysis on Experiments in Transformation of Deep-Water-Waves

Piotr Wilde

Institute of Hydro-Engineering of the Polish Academy of Sciences,
ul. Kościerska 7, 80-328 Gdańsk, Poland, e-mail: p_wilde@ibwpan.gda.pl

(Received December 30, 2004; revised April 08, 2005)

Abstract

The aim of the paper is to discuss the usefulness of the non-linear Schrödinger differential equation in the study of transformations of progressive deep water waves. Its solution compared with a regular Stokes type wave is essentially restricted to the first order approximation of the second one. The difference is that the Schrödinger equation introduces the concepts of a carrier wave and complex amplitude. In this way the dispersion relation of the third order Stokes expansion is taken into account. The analysis starts with regular, non breaking Stokes waves with large amplitudes as measured in our laboratory. The third order approximation is considered and compared with the corresponding solution of the Schrödinger equation. Then small periodic modifications are introduced in the time series fed into the control system of the generator. The approximation by trigonometric series is applied and the simplified analysis of superposition of very small modifications is used (higher powers of modifications are neglected). The Schrödinger non-linear equation is used in this analysis. The comparison of experimental and calculated envelopes is good, but for the surface elevations in space it is not as good. The approximation by trigonometric series is also applied to study the case of larger modifications. Finally the solutions of the Schrödinger equation corresponding to perfect solitons, are compared with the experimental data for cases where the measured surface elevations look almost like periodic solitons. This gives a reasonable approximation of the real behaviour in a very short space interval. It is not easy to get a good numerical description for the wave problem discussed as the waves are physically unstable. The results of the presented research will be used to establish an effective numerical procedure, stress the approximations introduced by the application of the Schrödinger differential equation and show how the theoretical solutions should be compared with the measured data.

Key words: water waves, stability, transformation, wave groups, non-linear Schrödinger differential equation

1. Introduction

Lighthill (1965) was one of the first to study the stability of motion problem for deep water waves. An important contribution is from Benjamin and Feir (1967).

They considered the basic frequency and a growth of the side frequencies when the wave progresses. Zacharov (1968) showed that the stability problem might be described by the non-linear Schrödinger differential equation. In his book, Witham (1974) described the properties of the dispersive waves. Important contributions to experimental research are due to Lake and Yuen (1977) and summarised in the book by Yuen and Lake (1982). Derivations of the non-linear Schrödinger differential equations for the description of deep water waves were proposed by other authors by different methods. Short descriptions of the basic properties and the Schrödinger differential equation are included to make reading of the paper easier.

The experimental research in transformations of deep water waves started at the Institute of Hydro-Engineering when the new 64 m long, 0.60 m wide and 1.40 m high wave flume was constructed. Precise experiments described in the paper by Wilde et al. (2003) were performed in our laboratory in the year 2001 and presented in detail in an internal report, Wilde et al. (2001). In the experiments, the wave trains were initiated by time series based on the algorithm presented by Wilde and Wilde (2001). The calculated time series was fed into the control system of the piston generator. The envelope of the horizontal motion grew slowly in time and was finally kept constant until the decay interval was introduced. The motion of the piston was fixed as the real part of the product of the values of the envelope as a function of time t with the function $\exp(-i\omega_d t)$, where ω_d was a fixed dominant frequency. In standard tests, surface elevations were measured by seven gauges denoted by S1...S7 that were placed at distances 4, 8, 16, 24,..., 48 m from the piston. Periodic modifications with very small amplitudes that resulted in the prescribed wave groups in time were introduced. In the present paper, fixed time intervals are discussed as they transform along the flume. The Eulerian description is used, and the surface elevations are measured by gauges along the flume.

In the theoretical analysis the approximations by trigonometric series are applied in the case of regular Stokes waves and in waves with superimposed small and finite modifications. The Kalman filter described in the book by Wilde and Kozakiewicz (1993) is used to decompose the measured data into two components. The first order components correspond to the neighbourhood of the dominant frequency and the second order components to the double of the dominant frequency. Such a decomposition is also applied to the Fourier components. The non-linear Schrödinger differential equation essentially describes the behaviour of the complex amplitude and is based on the first order approximation. The simple non-linear term in the Schrödinger differential equation takes care of the influence of the third order approximation on the dispersion relation. The second and third terms in the expressions for the surface elevations are neglected.

In the experiments, the modifications grew and in the middle of the flume looked almost like periodic solitons. They were not perfect solitons as they continued to change shapes along the flume, but in a small interval of space it is useful to approximate the measured surface elevation by the theoretical solution for a periodic soliton. The theoretical solution based on the non-linear Schrödinger differential equation was given in the paper by Martin et al. (1980). It is not possible to obtain a perfect approximation, but it is true that the Jacobi elliptic function *dn* is suitable when describing the motion of the envelopes. The experimental values corresponded to measurements by seven gauges placed at distances 40 m, 40.20, 40.40,. . . , 41.20 m from the piston. The spacing was so dense (0.20 m) as the measured surface elevations looked like solitons only in a small neighbourhood in space.

2. The Case of Regular Stokes Waves

In the wave flume, the amplitudes and frequencies of piston motions were controlled by time series fed into the control system of the generator. The depth of water h was equal to 0.6 m. In the experiments, it was assumed that the wave-length L (calculated according to the linear theory) was equal to $2h$, and thus it may be assumed that it is a deep water wave. In Fig. 4 of the paper P. Wilde et al. (2003) measured data of the transformation of a wave train are presented. The end parts of the data change significantly along the path of propagation, but the central part corresponds to a regular Stokes wave and is discussed in the present paragraph. The formulae for the third order deep water Stokes wave are the starting points of the analysis as they are given by Werhausen and Laitone (1960) by the relations (27.25), (27.26) and (27.27). These expressions are derived for the case the depth tends to infinity. The depth of water was not infinite, but when the dispersion relation for finite depth was used, the difference was around 1%. The surface elevation $\varsigma(x,t)$, the potential function $\Phi(x,z,t)$, and the dispersion relation is given by the following expressions:

$$\begin{gathered}
\varsigma(x,t) = A_d \cos(k_d x - \omega_d t) + \frac{1}{2} k_d A_d^2 \cos 2(k_d x - \omega_d t) + \\
+ \frac{3}{8} k_d^2 A_d^3 \cos 3(k_d x - \omega_d t), \\
\Phi(x,z,t) = A\sqrt{g/k_d} \exp(k_d z) \sin(k_d x - \omega_d t), \quad A_d = A\left(1 + \frac{1}{8} k_d^2 A^2\right), \\
\omega_d \cong \sqrt{g k_d}\left(1 + \frac{1}{2} k_d^2 A^2 \ldots\right),
\end{gathered} \tag{1}$$

where $\omega_d = 2\pi f_d$ is the angular frequency and f_d the frequency in Hz, k_d is the wave number, A_d is the amplitude of the first term in the expression for the

surface elevation, A is the amplitude that appears in the formula for the potential; it is related to the measured amplitude A_d by the expression given in the second row. If the amplitude A_d is very small then $A \approx A_d \to A_l$ the linear wave theory may be used and the wave number is related to the angular frequency by the formula $k_l = \omega_d^2/g$.

In the experiments, the seven gauges S1...S7 were placed at distances 4, 8, 16, 24, 32, 40, 48 m from the piston of the generator. For a fixed dominant frequency, three control time series of piston motions were fed into the control system of the generator by multiplication by three different factors. The largest factor corresponded to the case closest to breakage. The amplitudes of corresponding surface elevations [0.0204, 0.0285, 0.0362 m] measured by the gauge S3 were used as characteristic values for the progressive surface waves. In Fig. 1 the three frequencies measured on gauges S1 to S7 for the third case $A_d = 0.0362$ m are shown and compared with the mean values of the basic frequency and its double and threefold values $[f_d, 2f_d, 3f_d]$. The amplitude of the third component is very small, but still the estimated frequencies are almost constant along the flume. In all the experiments the values of frequencies changed very little along the flume and when the amplitude was increased. Thus it may be assumed that the measured frequencies stay constant, with values as given in the time series fed into the control system of the generator. The statistical values for all measured values are: for the basic frequency the mean value is 1.1390 Hz, the standard deviation 0.0010 Hz and for the second frequency the mean value is 2.2753 Hz and standard deviation 0.0067 Hz. The differences are well within the experimental accuracy.

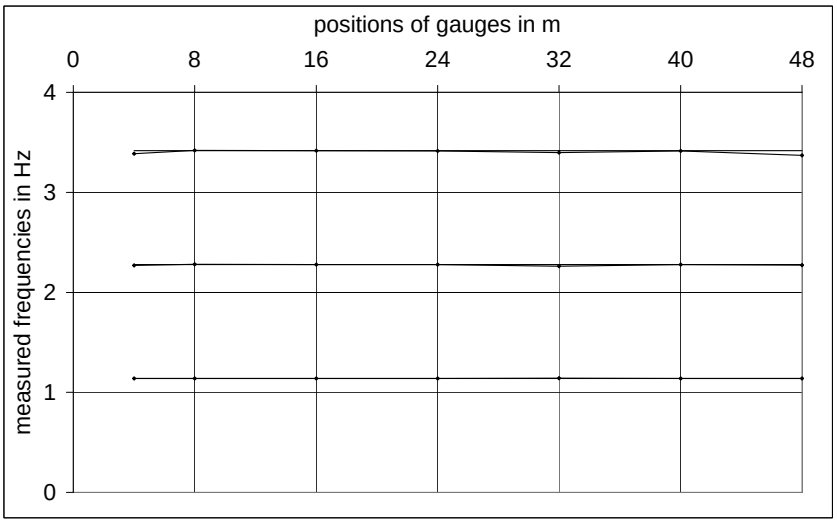

Fig. 1. Three frequencies measured along the flume and compared with mean values $f_d = 1.1390,\ 2f_d = 2.2780,\ 3f_d = 3.4170,\ a = 0.0362$ m

In Fig. 2 the amplitudes of the dominant frequency component as measured on gauges S1 to S7 are depicted with a least square approximation of the data by a straight line. It should be noted that the amplitudes in general decrease along the flume, but there are also oscillations with respect to the straight line approximation. These phenomena are mainly due to the dissipation of energy along the path of propagation. The wave motion is generated by the motion of the piston with uniform horizontal displacements along the depth of the water. In the region close to the piston of the generator the velocity profile changes to a negligible velocity at the bottom. This transformation is also accompanied by a dissipation of energy. Such behaviours can not be described by methods that do not describe damped progressive waves.

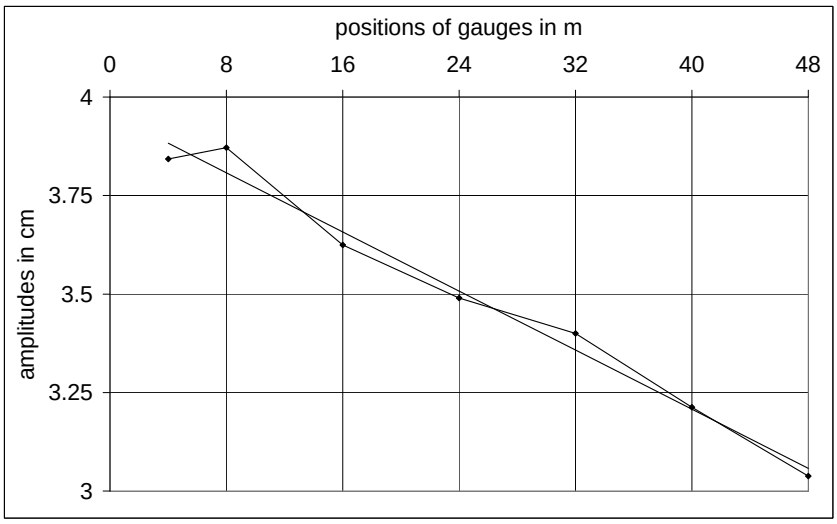

Fig. 2. Amplitudes of the first component measured by the seven gauges and approximation by a straight line, $a = 0.0362$ m

To calculate the value of the wave number k_d it is necessary to obtain the surface elevation as a function of distance x for a fixed time. In our laboratory an approximate graph may be obtained by a dense set of gauges with very small spacing. A theoretical local value may be calculated from the equations (1) as the solution of two non-linear equations: the dispersion relation and the relation between the amplitudes A_d and A with two unknown values A and k_d.

It is convenient to introduce the following dimensionless variables

$$x_A = A/A_d, \quad x_k = \sqrt{k_d/k_l} = \sqrt{k_d g}/\omega_d,$$

that transform these equation to the following form

$$\frac{1}{2}A_d^2\frac{\omega_d^4}{g^2}x_A^2x_k^5 + x_k - 1 = 0, \quad \frac{1}{8}A_d^2\frac{\omega_d^4}{g^2}x_k^4x_A^3 + x_A - 1 = 0. \tag{2}$$

The solution was constructed by successive approximations. It was assumed that initially $x_A = 1$ and this value substituted into the first equation makes it possible to calculate the value of x_k. There were five roots, two complex conjugate, but only one real. The real value substituted into the second equation led to the value of x_A (the real root) in the first step. Repeating the steps the successive approximations for the pairs $[x_k(r), x_A(r)]$, $r = 1, 2, \ldots$ were obtained. The convergence was very rapid. Four steps gave a very good accuracy. It should be mentioned that for our parameters the relative difference between A and A_d was around 0.25%. Thus it is reasonable to calculate the wave number from the dispersion relation with $A \approx A_d$

$$A_d^2 k_d^3 + k_d - k_l \cong 0, \quad k_l = \omega_d^2/g. \tag{3}$$

The difference between the calculated wave numbers is insignificant for parameters in our example.

In complex numbers the surface elevation of the Stokes wave is

$$\begin{gathered} \varsigma(x,t) = real(Z), \\ Z = A_d \exp[i\Theta(x.t)] + \frac{1}{2} k_d A_d^2 \exp[2i\Theta(x.t)] + \frac{3}{8} k_d^2 A_d^3 \exp[3i\Theta(x,t)], \end{gathered} \tag{4}$$

where $\Theta(x,t) = k_d x - \omega_d t + \varphi_0$.

The standard expression in real numbers is given in the first row of equations (1) and corresponds to the case the origin of the x, t coordinate system is at the maximum value $\xi(0,0) = A_d + k_d A_d^2/2 + 3k_d^2 A_d^3/8$ and thus $\varphi_0 = 0$. The general expression in complex numbers (4) corresponds to a shifted origin of the coordinate system. One must be careful in fixing the value of the angle φ_0. The complex expression (4) is convenient as the second term corresponds to the square of the first term multiplied by the coefficient $k_d/2$ and the third to the cube of the first term multiplied by $3k_d^2/8$. Thus, when the first term is known, the second and third terms may be easily calculated. This relation may be used in more general cases to obtain a reasonable estimate for the third order approximation.

A detailed analysis and comparison of calculated and measured values was done on one example by considering the case $A_d = 0.0285$ m (the middle one in the set) and restricting our attention to the surface elevations at the gauges S3, S4, S5, at distances 16, 24, 32 m from the piston. In this region, the influence of the region close to the piston is much smaller and thus the wave does not depend so much upon the way it is generated. The measured surface elevations were registered in the time interval 0.00–140.10 s with a sampling frequency 50 Hz (7006 data). For the gauges considered the data were transformed, so that they were accepted by the program MATLAB. The present analysis is restricted to the interval with no or very little influence of the starting and decay intervals and the

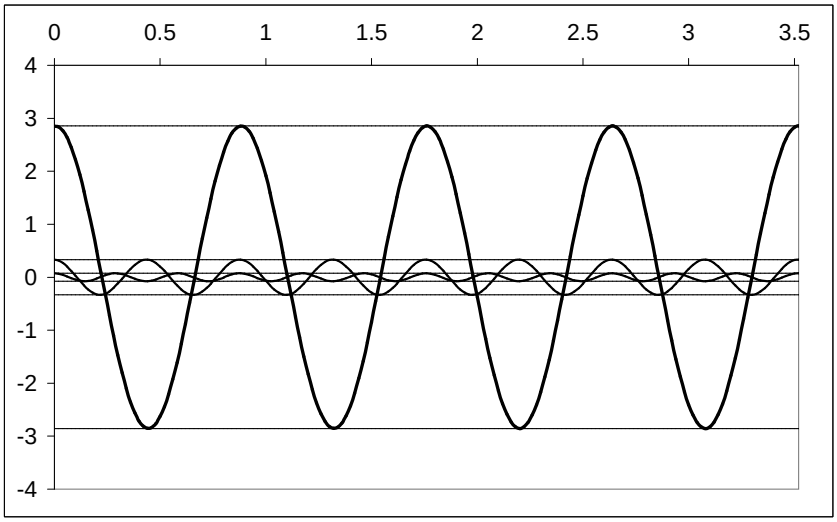

Fig. 3. Basic (amplitude 2.85 cm), double (amplitude 0.3330 cm) and threefold (amplitude 0.0748) Fourier components with envelopes, for the gauge S3

analysis is in a Eulerian description. Thus from the three data sets, time intervals of 84.48–89.76 s in length (265 data) were cut. The three Fourier components (coefficients and frequencies) were found by least square approximation for the measured surface elevations at S3, S4, S5. In Fig. 3 the three components with their envelopes are depicted for the measurements at S3. The first component has an amplitude equal to 2.85 cm the second 0.3330 cm and the third 0.0748 cm. A careful inspection shows that the addition of the double frequency term shifts the graph, the crests become steeper and the depth of the troughs decreases. The wave height does not change significantly. The third term has an influence on the wave height. It is small because its amplitude is very small. In engineering practise very often the linear theory is used, but it has to be remembered that to calculate the wave velocity the third order theory has to be used and when we are interested in the position of maximum wave crest the second term has to be considered. In Fig. 4 the three sets of graphs corresponding to the three gauges S3, S4 and S5 are depicted. The curves corresponding to the first order approximations have the corresponding amplitudes S3 2.85 cm, –2.85 cm, S4 2.7229 cm, –2.7229 cm and S5 2.6399 cm, –2.6399 cm. The sums of the three components, very close to the measured values have different upper and lower amplitudes. The corresponding envelopes were calculated as the absolute values of the three complex functions $Z_1,\ Z_2,\ Z_3$ corresponding to the three terms in the Eq. (4). The positions of the upper and lower envelopes z_{ue}, z_{le} were calculated according to the following formulae

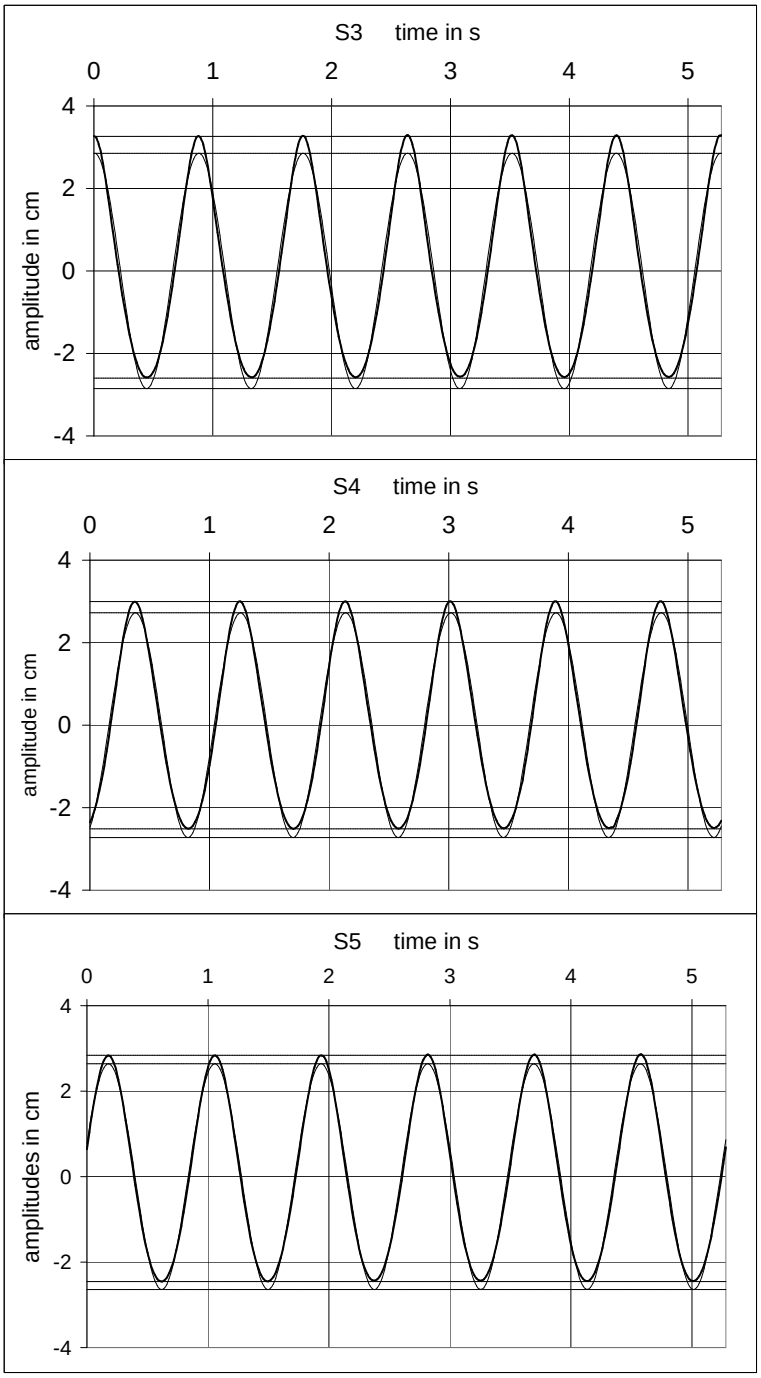

Fig. 4. Comparison of data measured and first order approximations for gauges S3, S4 and S5. Curves corresponding to the first order approximations have symmetric envelopes with amplitudes respectively 2.85, 2.72 and 2.64 cm. The sums of the three components have different upper and lower components

$$z_{ue} = abs(Z_1) + abs\,(Z_2) + abs\,(Z_3)\,,$$
$$z_{le} = -abs(Z_1) + abs\,(Z_2) - abs\,(Z_3)\,. \tag{5}$$

For the measured data the upper and lower amplitudes calculated according to the formulae (5) are S3: 3.2626 cm, –2.5966 cm, S4: 2.9994 cm, –2.5127 cm and S5: 2.8368 cm, –2.4572 cm. The surface elevations and the corresponding estimated upper and lower envelopes are depicted in Fig. 4. The relative errors between the first order approximations of the positions of the envelopes and the upper ones for the data at the three gauges are respectively 2.61%, 1.20% and 0.64%.

It may be seen that when the coefficients A_d, ω_d and in the expression for Z_1 are known, the positions of the upper and lower envelopes may be easily calculated and they are the envelopes for the measured surface elevations as function of time for the considered positions of the gauges.

The surface elevation as the function of distance x from the position of the gauge S3 and time t was also calculated by the relation (4). First, it was necessary, to calculate the wave numbers and the amplitudes k_d, and A for positions S3, S4, S5 as functions of the corresponding amplitudes A_d, by the successive approximations applied to the set of equations (2). The values of the surface elevation as the function of x for $t = 0$ are depicted in Fig. 5. In Fig. 6 the first order approximations of the surface elevations for positions of gauges S1, S2, S3 are shown. The decrease of wave height is small but visible. Solid lines indicate the measured values and envelopes, the calculated first term approximations are indicated by lines with crosses. It may be seen that there are phase shifts. The space interval of 16 m length spans 13 wave-lengths (average value around 1.23 m). The problem is how good the estimate of the wave-length is? If the error is just 1 cm, then the phase shift corresponds to 13 cm in 16 m. In general, in measured wave data, visible phase shifts are observed in comparison with theoretical solutions. In design the maximum values of surface elevations, frequencies and wave numbers are important. Thus from the engineering point of view, the knowledge of the envelopes, the values of the dominant frequency and wave number are important. Therefore the simplified description of water waves propagation as given by the non-linear Schrödinger differential equation is very interesting.

3. The Schrödinger Non-Linear Differential Equation

In the analysis of the transformation and stability of deep water waves, the non-linear Schrödinger equation, as given in the book by Yuen and Lake (1982)

$$i\left(A_{c,t} + v_g A_{c,x}\right) + \alpha A_{c,xx} - \beta |A_c|^2 A_c = 0 \tag{6}$$

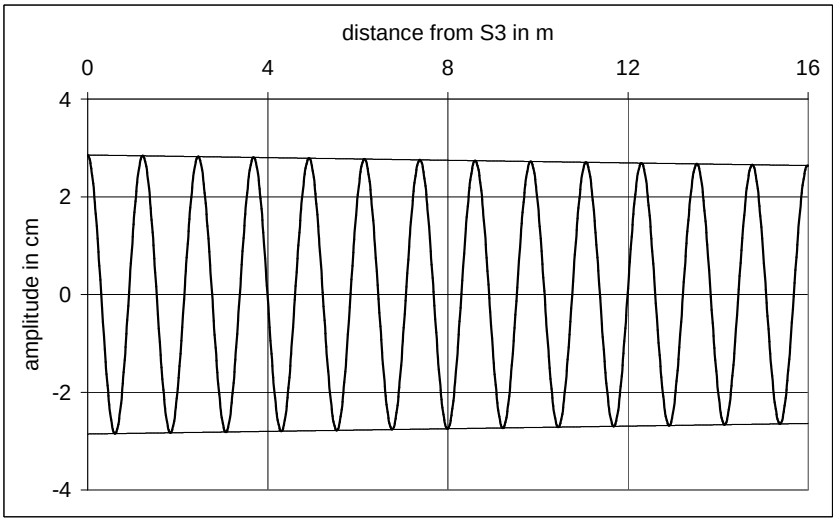

Fig. 5. Calculated surface elevations as functions of distance from S3, for $t = 0$

is used. In equation (6) A_c is the complex amplitude and the coefficients v_g, α and β are given by the following relations:

$$v_g = \frac{\omega_0}{2k_0}, \quad \alpha = -\frac{\omega_0}{8k_0}, \quad \beta = \frac{1}{2}\omega_0 k_0^2, \tag{7}$$

and quantities denoted by subscript 0 are the parameters of the carrier wave. When for a regular Stokes wave the parameters of the carrier wave correspond to the linear solution ($\omega_0 = \omega_l, \quad k_0 = k_l\,, \quad a \to 0$) then the Taylor series expansion of the dispersion relation is

$$\omega - \omega_l = v_g\,(k - k_l) + \alpha\,(k - k_l) + \beta a^2. \tag{8}$$

The coefficients are given by the expressions (7).

In the case of our experiments in the wave flume the dominant wave frequency is equal to the dominant frequency of the time series of piston motion fed into the control system of the generator. Thus it is convenient to take the carrier frequency equal to the dominant frequency $\omega_0 = \omega_d$ and to take the carrier wave number equal to the corresponding wave number when the amplitude tends to zero, that is $k_0 = k_l$ (the subscript l points to the linear theory solution, $k_l = \omega_d^2/g$).

For the case of a regular Stokes wave the dispersion relation is given by the corresponding expression in the equation (1), its approximate form (3), or its Taylor series expansion (8), and it is thus convenient to take

$$\begin{gathered}\omega_0 = \omega_d = \omega_l, \quad k_0 = k_l = \omega_d^2/g, \quad k_d - k_l = k_l\left(2 - 2\sqrt{1 + k_l^2 A_d^2}\right), \\ k_d - k_l \approx -k_l^3 A_d^2.\end{gathered} \tag{9}$$

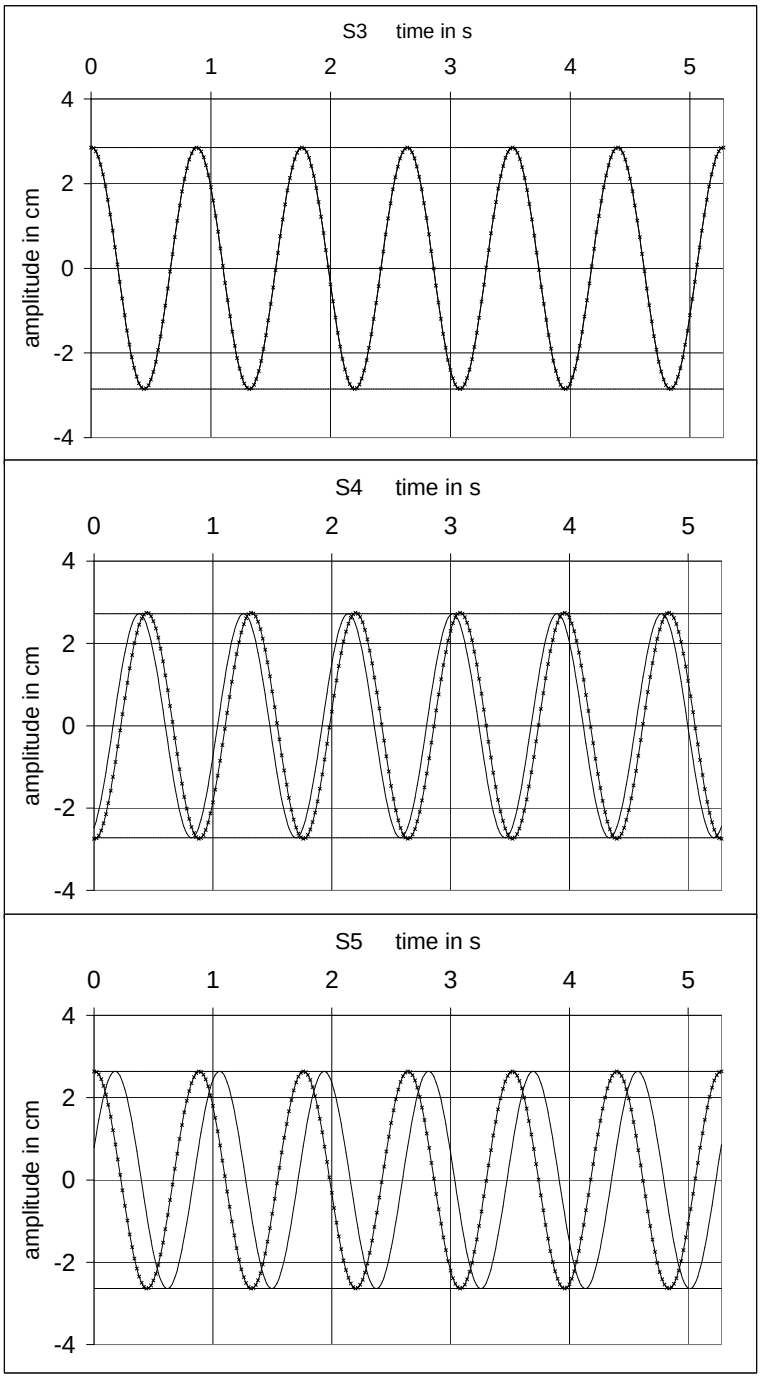

Fig. 6. Comparison of first order approximations for measured, solid lines and with x-marks calculated by Eq. (4), surface elevations at S3, S4, S5

The approximate relation follows from binomial expansion. The expression for the first term in complex notation for the complex amplitude of a regular Stokes wave, as given in the complex function notation given by the equation (4), may be written in the following form

$$Z = A_c(x)\exp\left[i\left(k_l x - \omega_d t + \varphi_0\right)\right], \quad A_c\left(x\right) = A_d \exp\left[i\left(k_d - k_l\right)x\right]. \tag{10}$$

The symbol $A_c(x)$ defines the complex amplitude for the regular Stokes wave. In this case, as in the wave flume, the dominant frequency in the time series introduced into the control system of the generator becomes the dominant frequency of the surface elevation. Thus this case may be called the frequency controlled case.

A second theoretical possibility is that the wave number is controlled. For the case of a regular Stokes wave it corresponds to the case

$$\begin{gathered} k_0 = k_d = k_l, \ \omega_0 = \omega_l = \sqrt{g k_d}, \\ \omega_d - \omega_l = \omega_l \left(-1 + \sqrt{1 + k_d^2 A_d^2}\right) \approx \frac{1}{2}\omega_l k_l^2 A_d^2. \end{gathered} \tag{11}$$

In this case, called the wave number controlled test, the corresponding complex amplitude is defined by the following relations

$$Z = A_c(t)\exp\left[i\left(k_d x - \omega_l t\right)\right], \ A_c(t) = A_d \exp\left[-i\left(\omega_d - \omega_l\right)t\right]. \tag{12}$$

It must be mentioned that in a standard wave flume it is not possible to control the wave numbers.

The non-linear Schrödinger differential equation is not restricted to the analysis of regular Stokes waves. In its derivation it is assumed that the amplitude is a function of distance and time $A_d = A_d\left(x, t\right)$, but that it is a modified regular Stokes wave. The modifications cannot be arbitrary, but, for example, by the addition of small terms to the basic regular Stokes wave. Such waves will be called Stokes-type waves.

The non-linear Schrödinger differential equation is a convenient relation for the description of Stokes type waves. It is a non-linear differential equation in complex variables, but there is only one simple algebraic non-linear term and for a regular wave, the variability of the real and imaginary parts is very slow as a function of distance ($k_d - k_l$ is a very small number when compared with k_d).

4. The Superposition of a Small Modification on a Stokes Wave

Let us consider the superposition of small modifications on the complex amplitude of a second order deep water wave given by the following expression:

$$
\begin{aligned}
A_c &= A_{c0} + \Delta A_c, \\
A_{c0} &= A_d \exp\left[-ik_d^3 A_d^2 x\right], \\
\Delta A_c &= \exp(Ux)\left\{\varepsilon_+ \exp\left[iK\left(x - v_g t\right)\right] + \right. \\
&\left. + \varepsilon_- \left[-iK\left(x - v_g t\right)\right]\right\} \exp\left[-ik_d^3 A_d^2 x\right].
\end{aligned}
\tag{13}
$$

In these relations A_{c0} is the complex amplitude of the regular Stokes wave, $K = k_l/n$ is the wave number of the wave group and n is the number of waves in the group in space (not necessarily an integer), $v_g = \omega_d/(2k_l)$ is the group velocity, the speed of energy propagation. It is assumed that the amplitudes of the modifications $\exp(Ux)\,\varepsilon_+$ and $\exp(Ux)\,\varepsilon_-$, small as compared with A_d, are so small that their products may be neglected. It is assumed that the amplitudes of the superimposed modifications may grow on the path of propagation by the term $\exp(Ux)$, where U has the dimension 1/m. In view of the relations (8), (9) and (13) it follows that the complex function description of the modified Stokes wave is

$$
\begin{aligned}
Z_1 = A_d \exp\left[i(k_d x - \omega_d t - \varphi_0)\right] &+ \exp(Ux)\,\varepsilon_+ \left[i(k_d + k_l/n)x - \right. \\
&\left. + i(1 + 1/(2n))\omega_d t - i\varphi_0\right] + \\
&+ \exp(Ux)\,\varepsilon_-\left[i(k_d - k_l/n)x - i(1 - 1/(2n))\omega_d t - i\varphi_0\right].
\end{aligned}
\tag{14}
$$

It should be noted that $Z_1(x,t)$ is just the first term of the generalised Stokes wave.

There are three additive terms in the relation (14). For a fixed distance x and for example $n = 3$ the three angular frequencies are respectively ω_d, $7\omega_d/6$ and $5\omega_d/6$. The groups in time have six wave periods. The picture in space, for a fixed time when $(k_l \approx k_d)$, is close to three additive terms with three wave numbers k_d, $4k_d/3$ and $2k_d/3$. This in general agrees with the experiments that the number of wave-lengths is equal to half the number of periods in a periodic group. In experiments, the behaviour of wave groups in time may be studied very precisely while it is not so easy to study this behaviour in space.

In the relation for the complex amplitude the value of the parameter U is not known. Its value has to be fixed from the condition that the function has to satisfy the Schrödinger differential equation (6) within the assumption that the modifications have very small amplitudes and the value of the parameter U is very small. Substitution of the modified complex amplitude (14) into the complex differential equation (6) leads finally to two homogeneous algebraic equations corresponding to the real and imaginary parts

$$\begin{bmatrix} \left(\frac{K^2}{8k_l^2} - k_l^2 A_d^2\right)\cos(K\xi) & -\frac{U}{2k_l}\sin(K\xi) \\ \frac{U}{2k_l}\cos(K\xi) & \frac{K^2}{8k_l^2}\sin(K\xi) \end{bmatrix} \begin{bmatrix} \varepsilon_+ + \varepsilon_- \\ \varepsilon_+ + \varepsilon_- \end{bmatrix} = \begin{bmatrix} 0 \\ 0 \end{bmatrix}, \tag{15}$$

where $\xi = x - v_g t$.

A non-trivial solution exists if the determinant of the equation is zero. This condition leads to the following equation for the unknown parameter U

$$\frac{U^2}{4k_l^2} = \left[k_l^2 A_d^2 - \frac{K^2}{8k_l^2}\right]\frac{K^2}{8k_l^2}. \tag{16}$$

The amplitudes of the modification grow if U is real, thus the value of K has to be in the interval

$$0 < K/k_l < 2\sqrt{2}k_l A_d. \tag{17}$$

The dimensionless parameter K/k_l is equal to 1/n. When the amplitude A_d tends to zero (linear wave) then K and U also tend to zero. The modifications do not grow. They grow if the following relation is satisfied

$$k_l A_d > 1/\left(2\sqrt{2}n\right).$$

A more detailed description of the stability problem is described in the paper by Wilde et al. (2003).

To obtain a large growth of modifications in experiments, one has to induce large amplitudes of the dominant wave, but one has to be careful to avoid such breaking waves that the description by the standard wave theory is not acceptable.

As an example, let us consider the results of an example described in the paper by Wilde et al. (2003) and depicted in their paper on page 302 in Fig. 7. In this example, the dominant frequency was $f_d = 1.1390$ Hz, the amplitude of the modifications was 5% of the regular wave and the number of waves in a group in time was 6 (in space $n = 3$). To compare the experimental data with the solution of the Schrödinger differential equation proposed in this paragraph it is necessary to restrict the analysis to the case of small modifications. Calculations showed that for the measurement at positions S1 (4 m), S2 (8 m) and S3 (16 m) it was necessary to consider the first order components with the dominant frequency and the two side frequencies $[5f_d/6,\ f_d,\ 7f_d/6]$ and the second order components $[11f_d/6,\ 2f_d/6,\ 13f_d/6]$. Thus the first order components conform to the assumed form of the solutions (11) and (12) of the Schrödinger differential equation. The part of the measured surface elevations that corresponded to the same

time interval for all gauges was decomposed into a trigonometric series by a least square approximation. In Fig. 7 are depicted three graphs, the first shows the dominant component, the second the sum of side components and the third, a dotted line, the first order approximation. This figure illustrates the properties of the first order components based on the measurements by the gauge S1 and corresponds to the initial value in space for the progressive waves. In Fig. 8 the corresponding components are depicted for the measurements at S3. It is worthwhile noting that the sums of side components have a period equal to 6 dominant wave periods and that the modifications grow, but are still small at S3.

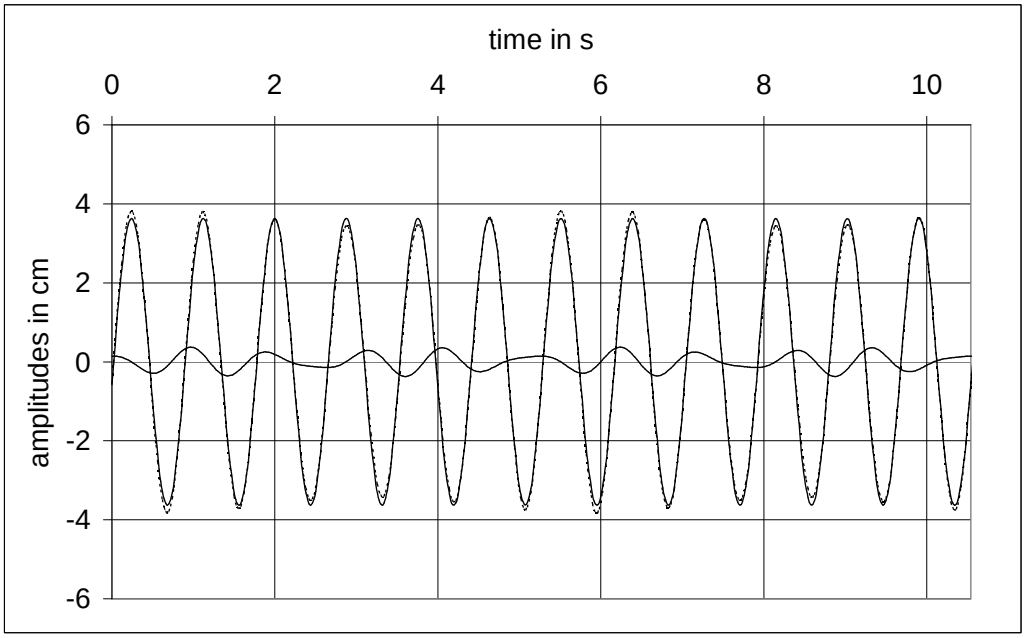

Fig. 7. Dominant component, sum of side components – solid lines and dotted line – the first order approximation, sum of three components at gauge S1

The propagation distance from the gauge S1 to S3 was divided into small steps of length $\Delta x = 0.02$ in m. The surface elevations measured by gauges S1 to S5 were used to obtain a second order polynomial approximation of the amplitudes as the function of distance. The dispersion relation was used to obtain the relation of wave numbers as the function of distance. The wave parameters at S1 were used as initial values to calculate the value of U according to the relation (16). In the very small step the exponential function may be replaced by its expansion $\exp(U\Delta x) \cong 1 + U\Delta x$. The values of the wave number and amplitudes at $x = 0$ become $k_d(\Delta x)$, $A_d(\Delta x)$, $(1 + U\Delta x)\varepsilon_+$ and $(1 + U\Delta x)\varepsilon_-$ at the end of the first interval and are the initial values for the second interval. Repeating the consecutive steps the values of the three first order components are obtained.

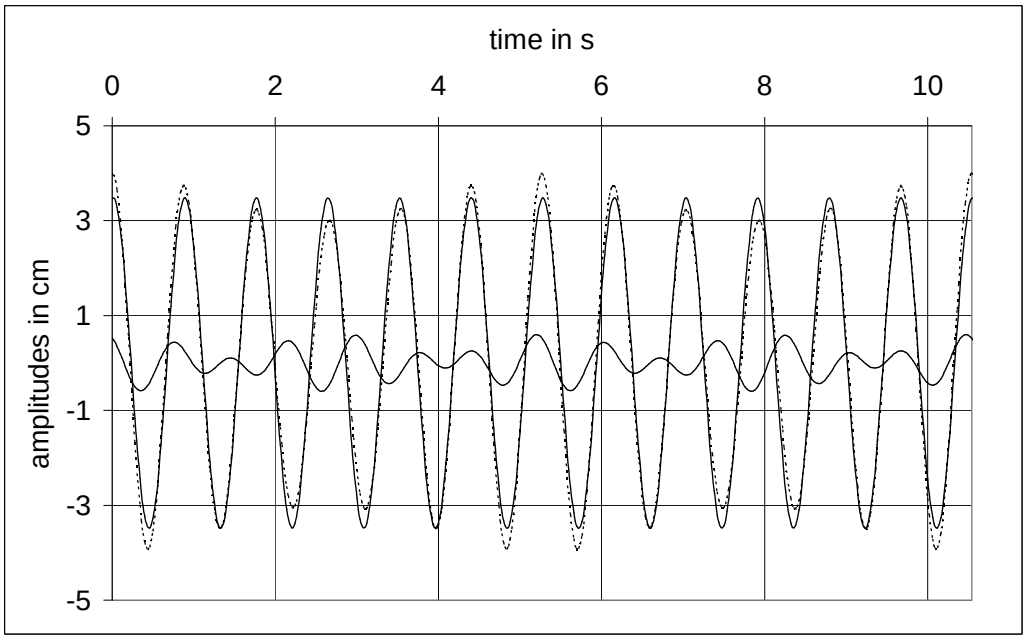

Fig. 8. Dominant component, sum of side components – solid lines and dotted line – the first order approximation, sum of three components at gauge S3

The calculated graphs are depicted in Fig. 9. The first order approximation (the sum of the three components) and the envelopes are depicted in Fig. 10. It should be noted that the calculated envelopes are symmetric with respect to the reference x axis.

The measurements of surface elevations show that the peaks are steeper and the troughs milder, as in the Stokes waves. Let us consider the influence of the second order approximations. The surface elevations measured by the gauges may be used to calculate the second order frequencies and their corresponding Fourier series coefficients. Thus neglecting the third order terms we can calculate the surface elevation within the second order approximation at the positions of the gauges as

$$Z_m(x_r, t) \cong Z_1(x_r, t) + Z_2(x_r, t), \tag{18}$$

where $Z_m,\ Z_1,\ Z_2$ are respectively the measured, the first and second order approximations by Fourier series. The third order approximations may be taken into account, but when the amplitudes of the higher terms become very small it is not worthwhile doing it. Now it is possible to calculate the positions of the upper and lower envelopes by the two terms in the relations (5). These functions calculated for the data of the gauge S3 are depicted in Fig. 11 by thicker lines.

When the modifications are small compared with the amplitude of the dominant wave we may generalise the expression for the Stokes wave (4) and estimate the second order term by

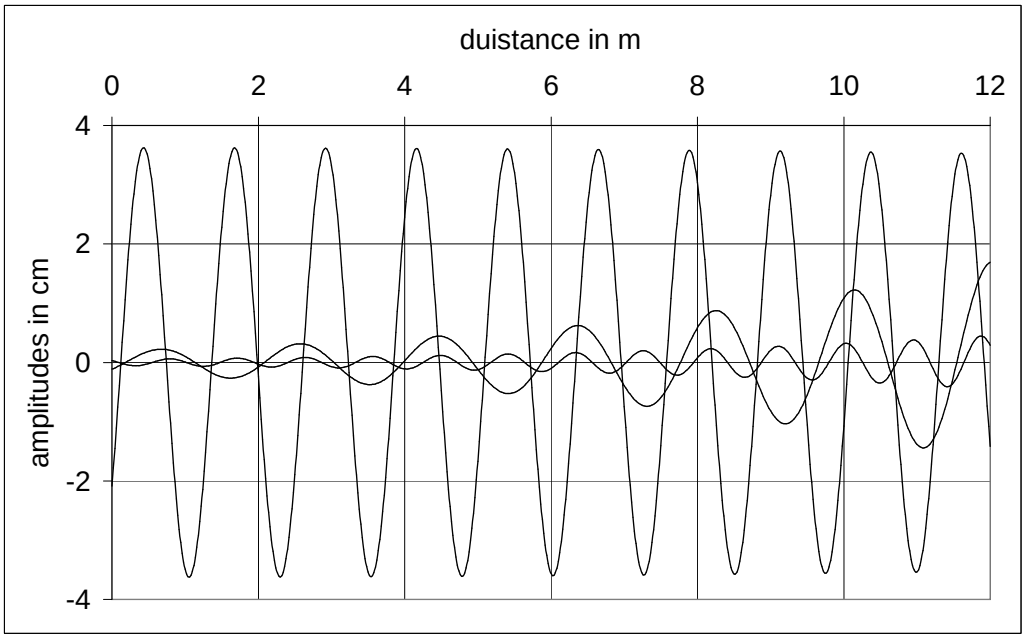

Fig. 9. Calculated three first order surface elevation components in the interval from S1 to S3 as function of distance from the gauge S1

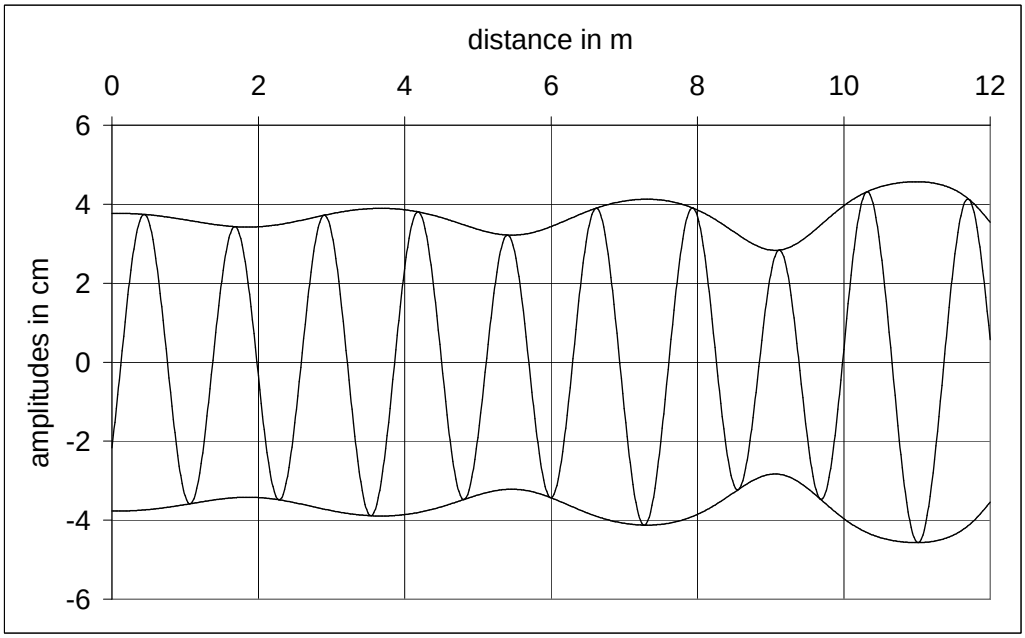

Fig. 10. First order approximation of calculated surface elevations and envelopes in the interval from S1 to S3

$$Z_2(x_r t) \approx \frac{1}{2} k_d Z_1^2(x_r, t) . \tag{19}$$

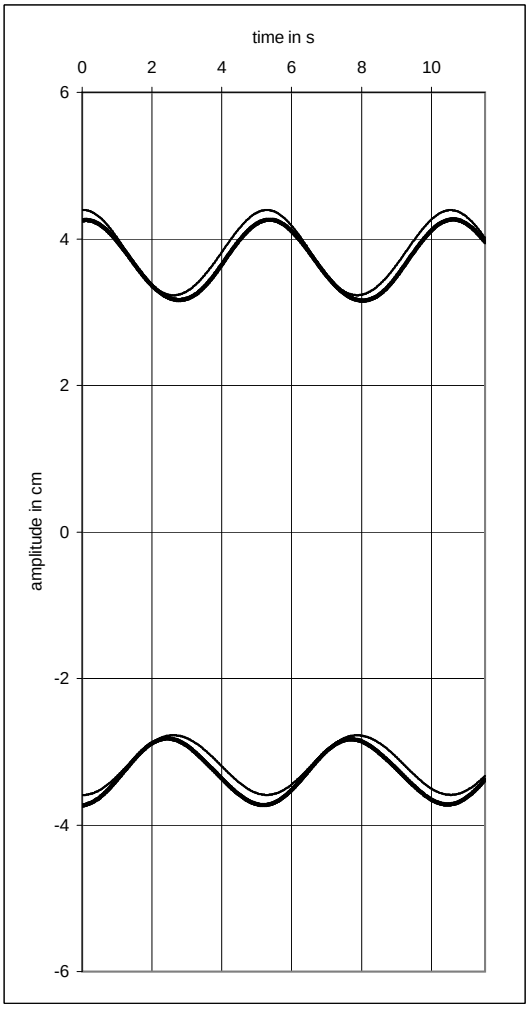

Fig. 11. Measured with included measured second order terms (thicker lines) and estimated within second order approximation (thinner lines) envelopes for the gauge S3 as a functions of time

The corresponding estimated upper and lower envelopes for the gauge S3 are shown in Fig. 11 by thinner lines. There are differences, but the estimate based on the knowledge of the first order surface elevation is a good one for practical applications. It must be remembered that a solution based on the non-linear Schrödinger differential equation considers in detail only the first order terms in the description.

5. An Approximation by Fourier Series for Finite Modifications

The assumption that the modifications are small is not true when, due the transformation along the path of propagation, the modifications become finite. In the experiments, Wilde et al. (2001), the surface elevations as functions of time were measured in the interval 40 to 41.2 m by seven gauges in 0.20 m spacing. Approximation by trigonometric series was applied to the measured data in the least square sense. The starting point was the Fourier analysis applied to a constant time interval corresponding to the periodic part of the data. The length of the data interval was adjusted to obtain a small number of important components. The adjusted time interval was used to obtain the best approximation for all surface elevations measured by the seven gauges. For the data measured by seven gauges the statistical values for the frequencies in Hz are presented in Table 1. The standard deviations show that the differences for different gauges are well within an experimental error. It may be assumed that the considered set of data has constant frequencies given by the set

$$F = [5/6,\ \ 1,\ \ 7/6,\ \ 8/6,\ \ 9/6,\ \ 11/6,\ \ 12/6,\ \ 13/6]\, f_2. \tag{20}$$

Table 1. Mean values, standard deviations and relative frequencies with respect to $f_2/6$

mean f_s	0.9460	1.1370	1.3272	1.5173	1.7029	2.0870	2.2759	2.4587
std f_s	0.0012	0.0003	0.0009	0.0029	0.0082	0.0117	0.0061	0.0084
mean $6f_s/f_2$	4.9921	6.0000	7.0038	8.0069	8.9862	11.0179	12.0098	12.9746

The amplitudes of the components as measured by the seven gauges, are depicted in Fig. 12 and the corresponding phases in Fig. 13. The amplitude of the component with the relative frequency 10/6 was very small and neglected. The first five components correspond to the first order approximation (linear theory). The following three correspond to the second order approximation. There are higher frequency components, but the presented analysis is concerned with a description as given in the Schrödinger differential equation where the discussion is mainly restricted to the first order approximation.

It is reasonable to replace the amplitudes by their mean value. It is not obvious whether the discrepancies are due to the physics of the problem or experimental errors. The phases of the components as functions of distance may be approximated by straight lines. The slopes correspond to wave numbers of the components and the values for $x = 0$ to the initial angles $\varphi_s\,(0)$ at the position S1. In the experiments, the introduced small modifications had amplitudes equal to 5% of the dominant values. It must be noted however, that the progressive wave at a distance of 40 m from the piston is the result of transformations over a large distance. The first order approximations of the measured surface elevation and their envelopes by the gauge S1 (distance 0.40 m) are depicted in Fig. 14 by the thinner lines. The corresponding graphs based on measured data by the gauge S3 (distance 40.40 m)

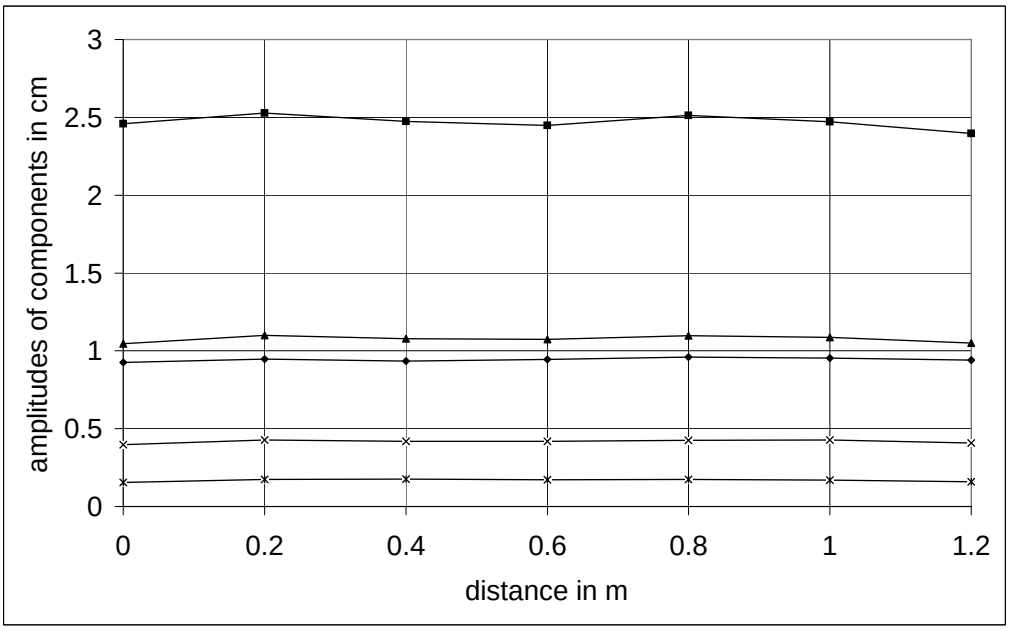

Fig. 12. Amplitudes of components as measured by the seven gauges in cm
$f_1 = 0.9460$ Hz, $f_2 = 1.1370$ Hz, $f_3 = 1.3272$ Hz, $f_4 = 1.5173$ Hz, $f_5 = 1.7029$ Hz

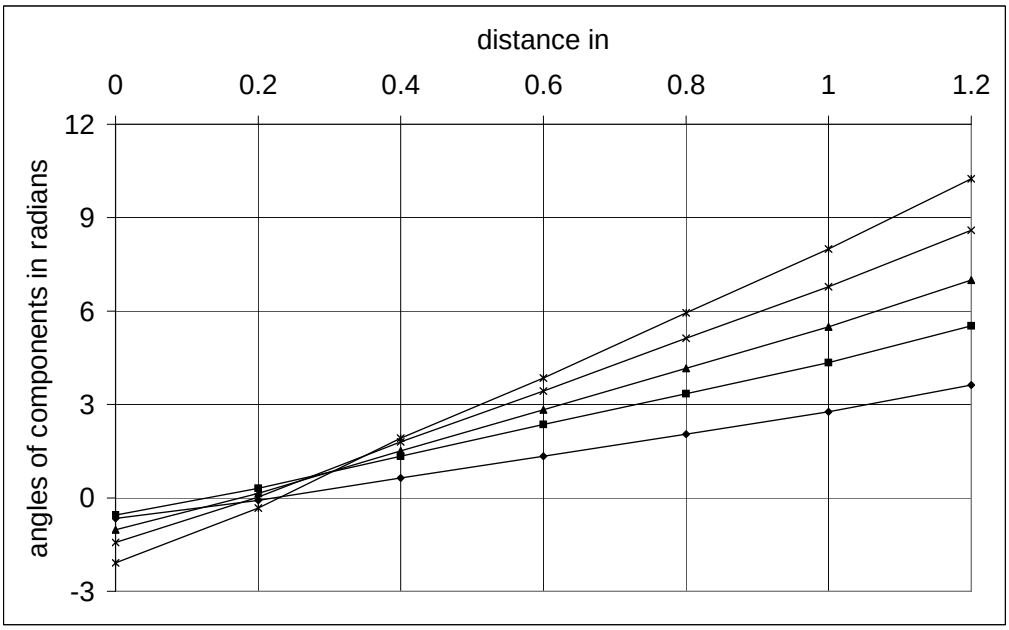

Fig. 13. Phases of components as measured by the seven gauges in radians
$f_1 = 0.9460$ Hz, $f_2 = 1.1370$ Hz, $f_3 = 1.3272$ Hz, $f_4 = 1.5173$ Hz, $f_5 = 1.7029$ Hz

are shown by thicker lines. It may be seen that the path of motion of the peak of the envelope from position S1 to S3 is approximately one half the length of the path of the crest of the wave.

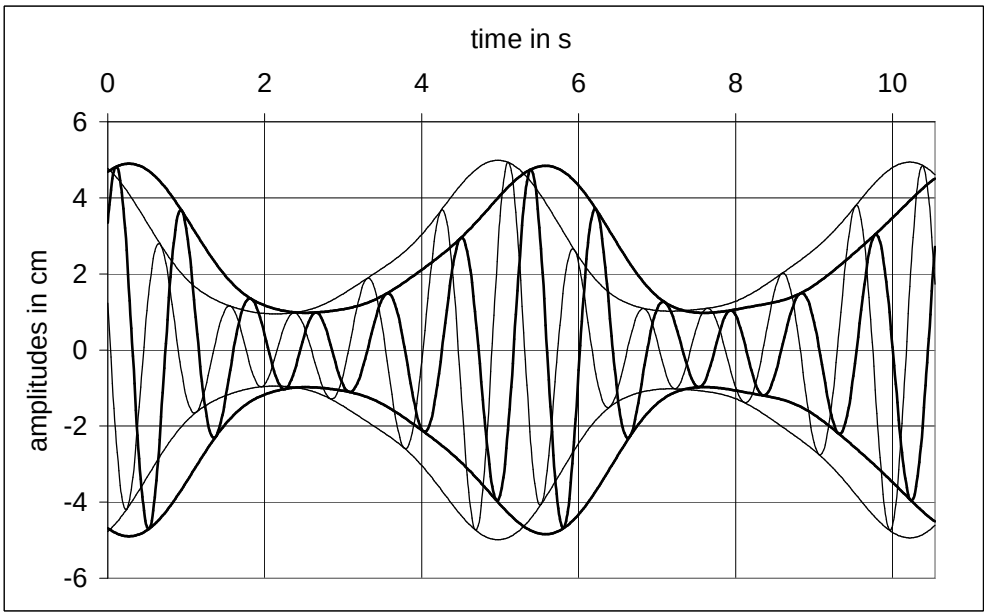

Fig. 14. First order approximations at gauges S1 (thinner lines) and S3 (thicker lines) as functions of time, distance 0.40 m

The seven upper envelopes corresponding to the measurements by the seven gauges as functions of time are depicted in Fig. 15. There is a substantial regularity in the graphs. It is difficult to say which differences are due to experimental errors and which due to physical phenomena.

Let us discuss the surface elevations as functions of distance along the flume. Unfortunately, in our laboratory we have no possibility of measuring the surface elevations as a function of distance x at fixed times. In the present paper it is possible to base these discussions on data measured by seven gauges looking for local approximations as mean values and approximation of phases by straight lines. The slopes of the graphs of the phases (Fig. 13) correspond to the wave numbers of components. These values are presented in the first row of Table 2. The ratios of the consecutive wave numbers with the second one and multiplied by three are presented in the second row. These dimensionless numbers are close to integers and thus it is possible to obtain estimated values of wave numbers corresponding to the first order approximation of the frequencies given by the five first ones in the set (20). To relate these values to the description by the non-linear Schrödinger differential equation it is only necessary to calculate the linear dominant wave number according to the formula

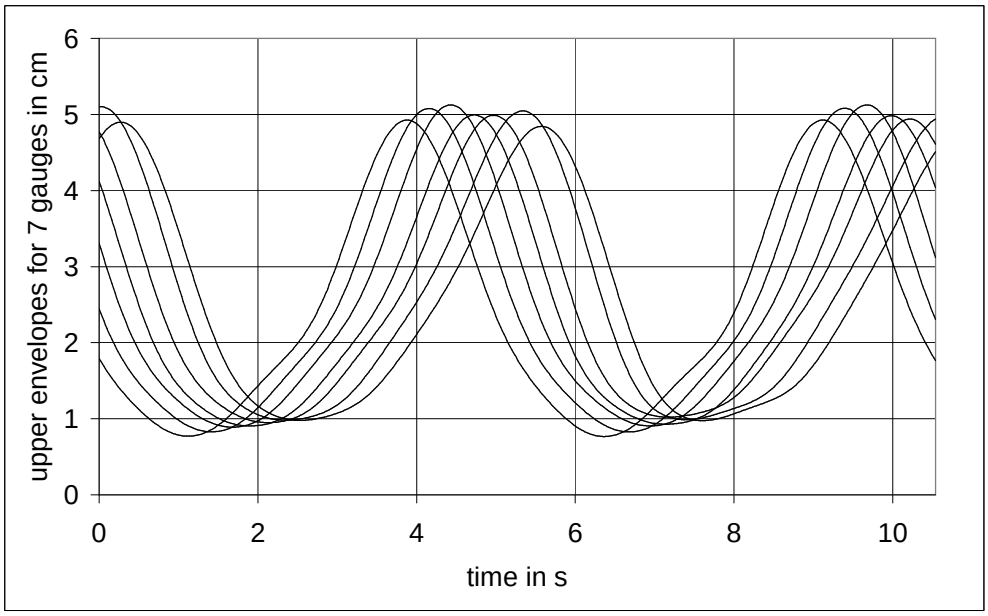

Fig. 15. Set of upper envelopes in first order approximation for the seven gauges S1 to S7 (spacing 0.20 m) as functions of time

$$k_{ld} = \omega_d^2/g.$$

The estimated values are given in the third row of Table 2.

The choice of the set of integers depends upon the choice of the set of frequencies that correspond to the description by the linear theory. It should be noted that the comparison of Table 2 with Table 1 shows that the introduced simplifications in the case of wave numbers are not so close to the measured ones as in the case of frequencies.

Table 2. Experimental and estimated wave numbers of main components

Experimental wave numbers k_s	3.5626	5.0601	6.6796	8.3812	10.2965
Dimensionless values $3k_s/k_2$	2.1122	3.0000	3.9601	4.9690	6.1045
Estimate [2, 3, 4, 5, 6] $k_{ld}/3$	3.4689	5.2026	6.9368	8.6710	10.2965

The surface elevation and the corresponding envelopes as functions of distance from the first gauge (while $t = 0$) are depicted in Fig. 16. These calculated graphs are based on the introduced simplifications. It may be seen that the number of waves in the period of the envelope is almost equal to three. It should be noted that the experimental values are restricted to the interval 0–1.20 m. The remaining part is based on estimated parameters.

In the assumed spacing of the gauges (20 cm) it is reasonable to assume that the amplitudes of components are constant and that the phases as the function of x

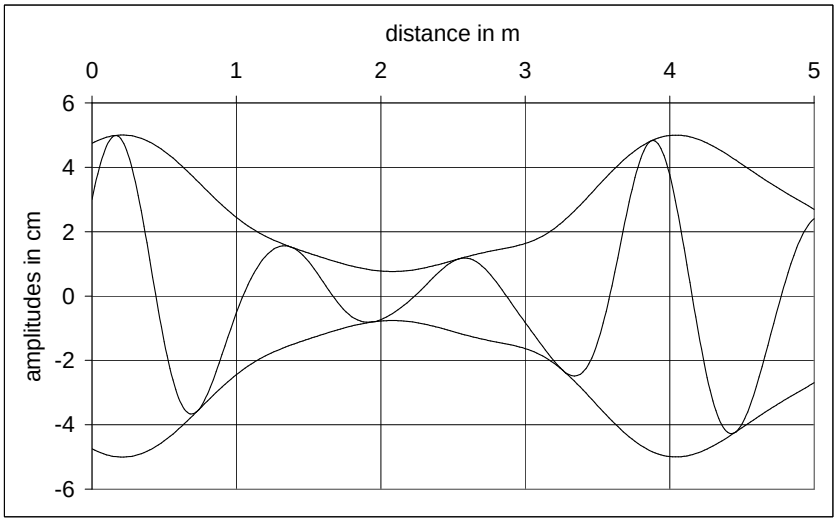

Fig. 16. Calculated first order approximation of elevations and envelopes as function of distance from the gauge S1 in space

for a constant t may be approximated by a straight line and thus the wave numbers are constant. These statements are true for the investigated interval of 1.20 m length. There is a dissipation of energy along the path of propagation of the wave in the flume. Thus the amplitudes of the components and the wave numbers must change as a function of distance. The discussed example shows that the applied spacing is good and would be satisfactory to obtain the experimental values of amplitudes and wave numbers along the flume. To obtain it, one should measure the surface elevations by at least 200 gauges in 100 Hz sampling frequency. The laboratory is equipped to register such an amount of data. The problem is in the cost of gauges and the necessary installations. If such measurements were available it would be possible to calculate the complex amplitude based on the experimental values.

6. The Periodic Solitons

In the experiments the initially small modifications grew along the path of propagation, then the growth decreased and it looked like an almost periodic soliton with wave groups moving with group velocity and dominant wave moving with phase velocity. In Fig. 17 the graph of four wave groups as functions of time (with six waves in a group) cut from a much longer record of measured data is presented. This graph corresponds to surface elevation measured by the gauge placed at a distance of 40.20 m from the piston of the generator. The measurements were decomposed into two components by a Kalman filter as introduced by Wilde and Kozakiewicz (1993). The components correspond to the peak frequency (first order) and to the double of the dominant frequency (second order)

and are depicted in Fig. 18. It should be noted that the second order components increase the maximum positive values and decrease the depths of the troughs. The phenomenon is the same as in the case of regular Stokes waves. The Schrödinger differential equation (5) describes only the first order component, thus only components in the neighbourhood of the dominant frequency are considered.

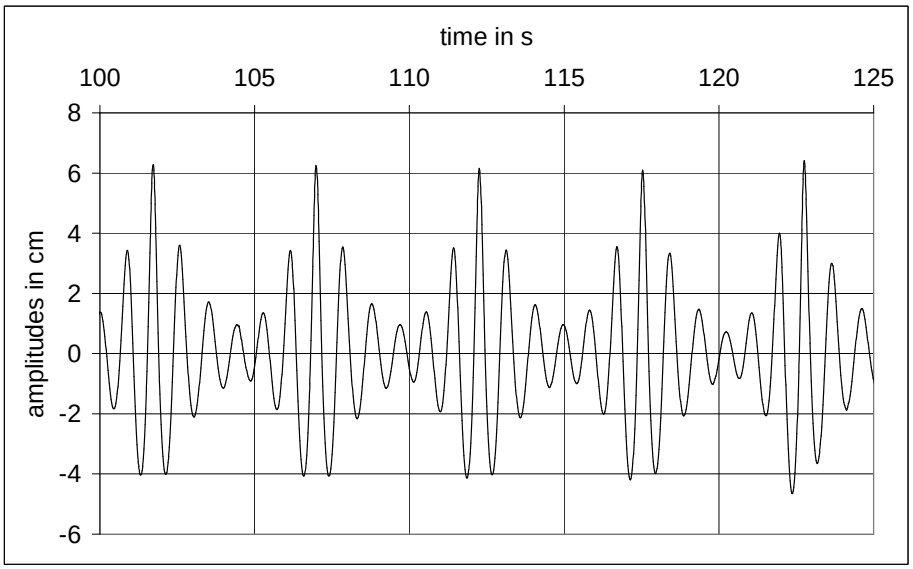

Fig. 17. Measured surface elevation, four wave groups at S7, distance 41.20 m from piston

Martin et al. (1980) presented the analytical expression for the periodic soliton of the non-linear Schrödinger differential equation (6). A short description of Martin's solution will be given for the case as given by the expressions (12) to (17) in the paper by Wilde et al. (2003). Let us write the transformation of variables (Martin et al. 1980) in matrix notation with the corresponding inverse transformation

$$\begin{bmatrix} T \\ X \end{bmatrix} = \begin{bmatrix} -\omega_l & 0 \\ -\omega_l & 2k_l \end{bmatrix} \begin{bmatrix} t \\ x \end{bmatrix}, \quad \begin{bmatrix} t \\ x \end{bmatrix} = \begin{bmatrix} -\omega_l^{-1} & 0 \\ -(2k_l)^{-1} & (2k_l)^{-1} \end{bmatrix} \begin{bmatrix} T \\ X \end{bmatrix}. \tag{21}$$

where T and X are dimensionless variables.

The transformation leads to a simple form of the Schrödinger non-linear differential equation in the dimensionless unknown function $B(X, T)$ that is proportional to the complex amplitude $A_c(X, T)$ (the function $A_c(x, t)$ with new variables), $B(X, T) = A_c(X, T)\, k_l/\sqrt{2}$

$$i B_{,T} + \frac{1}{2} B_{,XX} + |B|^2 B = 0. \tag{22}$$

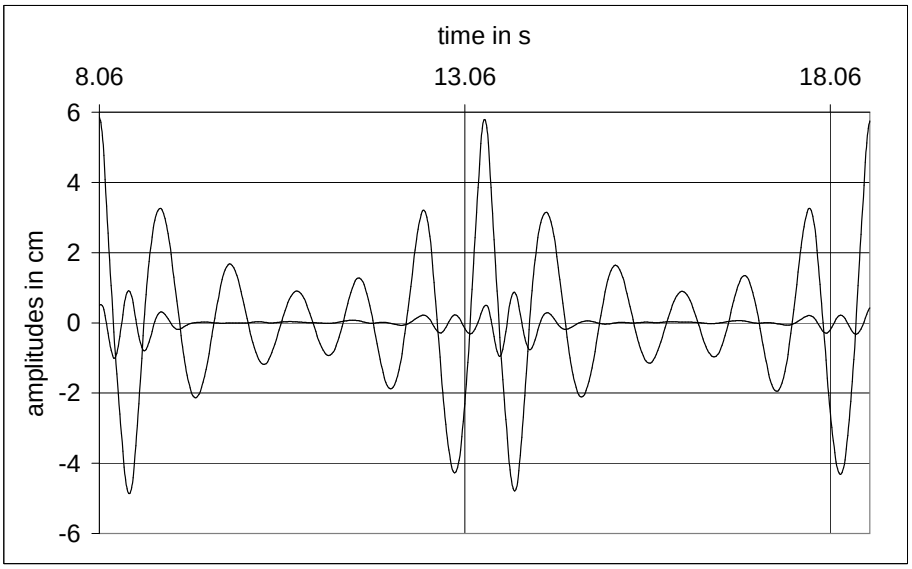

Fig. 18. Decomposition into first and second order components by Kalman filter (two groups presented). The curve with bigger values corresponds to the dominant frequency 1.1370 Hz, the second to the dominant frequency 2.2740 Hz

The separation of variables gives

$$B(X, T) = \Phi(X) \exp\left(i\gamma^2 T\right), \tag{23}$$

where γ is a dimensionless real number and leads to the following second order differential equation for the dimensionless function $\Phi(X)$:

$$\frac{1}{2}\Phi_{,XX} - \gamma^2\Phi + \Phi^3 = 0. \tag{24}$$

The differential equation (24) has a periodic solution expressed by the Jacobi elliptic function

$$\Phi(X) = \beta_p dn\left[\beta_p X, m\right], \tag{25}$$

where the parameters β_p and m are dimensionless real numbers, $0 \leq m \leq 1$ and $\beta_p = \gamma\sqrt{2/\left(2 - m^2\right)}$.

To discuss the meaning of the solution let us go back to the variables x, t by the transformation of variables (21) and the relation between the complex number solution (12). The surface elevation as calculated by the non-linear Schrödinger equation is the real part of the complex number solution

$$\xi(x, t) = \frac{\sqrt{2}}{k_d}\beta_p dn\left[\beta_p\left(2k_l x - \omega_l t\right), m\right] \cos\left[k_l x - \left(1 + \gamma^2\right)\omega_l t + \varphi_0\right]. \tag{26}$$

This solution (26) describes a progressive wave with a variable in space and time amplitude. The progressive wave moves with phase velocity and the periodic amplitude moves with a group velocity that is approximately one half of the phase velocity.

The dominant wave has the dominant wave number k_l and the dominant frequency

$$\omega_d = \left(1 + \gamma^2\right) \omega_l. \tag{27}$$

The function $dn\left[\beta_p\,(X - X_0)\right]$ is equal to one for $X = X_0$ and for all arguments corresponding to the multiples of the period. For other arguments its value is less than one, but not negative. It follows from the relation (26) that the coefficient $\sqrt{2}\beta_p/k_d$ is equal to the maximum value of the amplitude $A_{\max}$, hence

$$\beta_p = k_d A_{\max}/\sqrt{2}. \tag{28}$$

The parameter m may be fixed from the measured number of periods in the periodic group in time. It is well known that the period of the Jacobi elliptic function is equal to twice the value of the complete elliptic integral $K(m)$ and thus the number of waves in a group in time n_t is

$$n_t = 2K\,(m)\,/\left(2\pi\beta_p\right). \tag{29}$$

In the considered experiments there are no data that correspond to a perfect periodic soliton. The experiments described in Chapter 6 have features that in small intervals of time and space are close to the behaviour of a periodic soliton. Let us estimate the parameters that enter the description. The parameters estimated from the experimental data with values for the example are: the dominant frequency $f_d = 1.1390$ Hz and ω_d, amplitude $A_{\max} = 0.055$ m, the number of waves in a group in time $n_t = 6$. The parameters that enter the relations for a periodic soliton are $\omega_l, \beta_p, m, \gamma$ and k_l. Now $k_l = \omega_l^2/g$, γ may be calculated from the relation (27), the parameter β_p may be calculated from the relation (28), the same β_p may be calculated from the relation in (25) when the parameter m is known. These values must be equal. This condition leads to the following algebraic equation

$$\frac{2 - m^2}{4}\frac{a_{\max}^2}{g^2}\omega_l^5 + \omega_l - \omega_d = 0. \tag{30}$$

In this equation there are two unknowns ω_l and m. To calculate them we have to use the relation (29) where the number of waves in a group in time is known. The value of m has to be assumed. The equation (30) has five roots, four complex conjugate and one real. When the value of ω_l is calculated it is possible to find all the other parameters. A new value of m has to be chosen and the calculations

repeated. Successive approximations have to be applied to find both unknowns that satisfy the two algebraic equations.

A numerical example, based on assumed values of parameters, was calculated. The calculations yielded the following values of parameters $m = 0.9887$, $n_t = 5.9977$, $f_l = 1.1172$ Hz and $\beta_p = 0.1954$, $\gamma = 0.1395$.

In Fig. 19 the calculated elevations and envelopes are depicted as functions of time. The comparison with the measured values as presented in Fig. 17 show that these surface elevations have different positions of upper and lower envelopes. When the average value is taken then the agreement with the theoretical solution based on the solution of the non-linear Schrödinger equation is good.

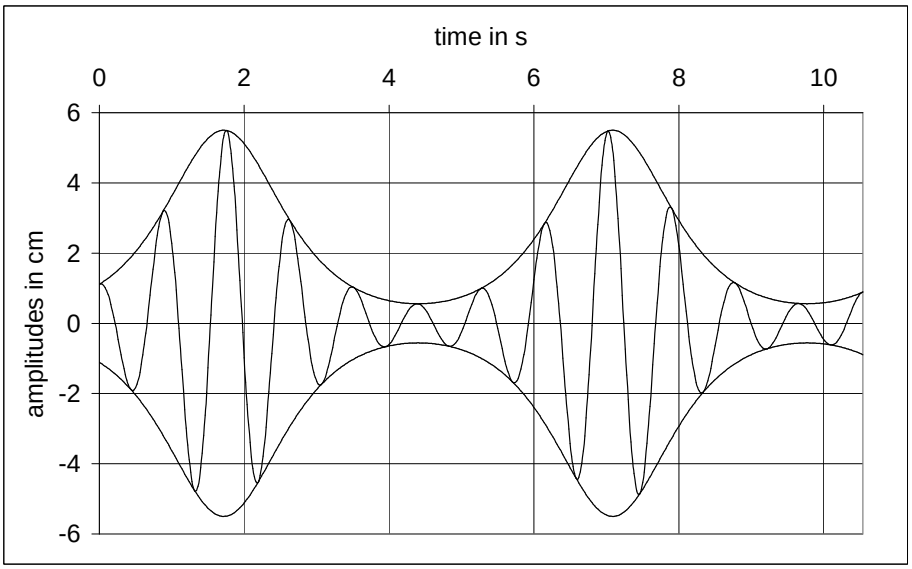

Fig. 19. Elevations and envelopes at S7 as function of time calculated as the corresponding periodic soliton

The envelopes corresponding to seven positions with (spacing 0.20 m) as functions of time are depicted in Fig. 20. The comparison of corresponding graphs based on measurements (Fig. 15) shows that the graphs based on the solution for periodic solitons confirm the real behaviour and correspond to an idealised theoretical description.

In Fig. 21 the envelopes and elevations as functions of distance that correspond to the solution for a periodic soliton are presented. The correspondence is reasonable and in the group in space there are around three wave-lengths. It must be mentioned however that the considered distance here was 1.2 m and the spacing was 0.20. In experiments these waves were not stable in greater space intervals and the transformation on the path of propagation was essential. It must be stated that comparison of the theoretical solution for a perfect soliton may

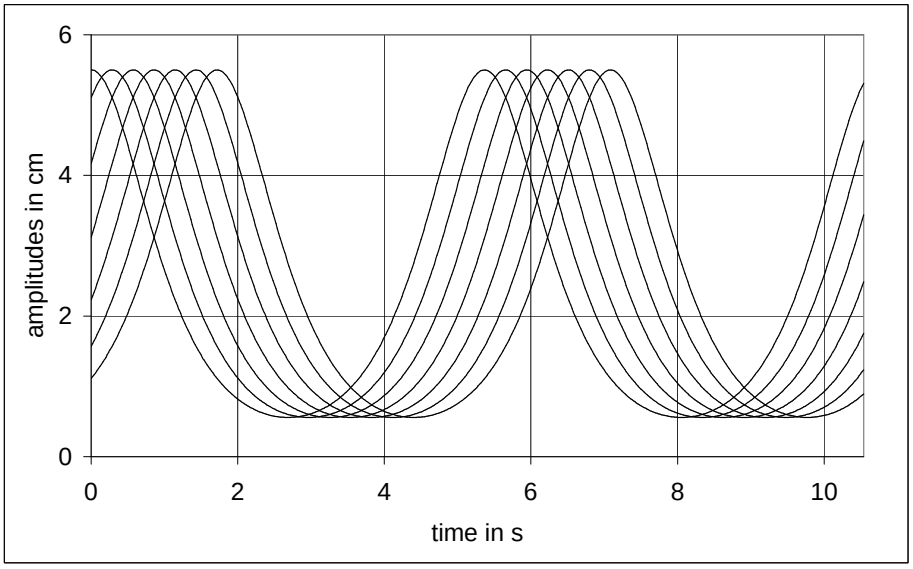

Fig. 20. Set of envelopes (spacing 0.20 m) as functions of time for the corresponding perfect periodic soliton

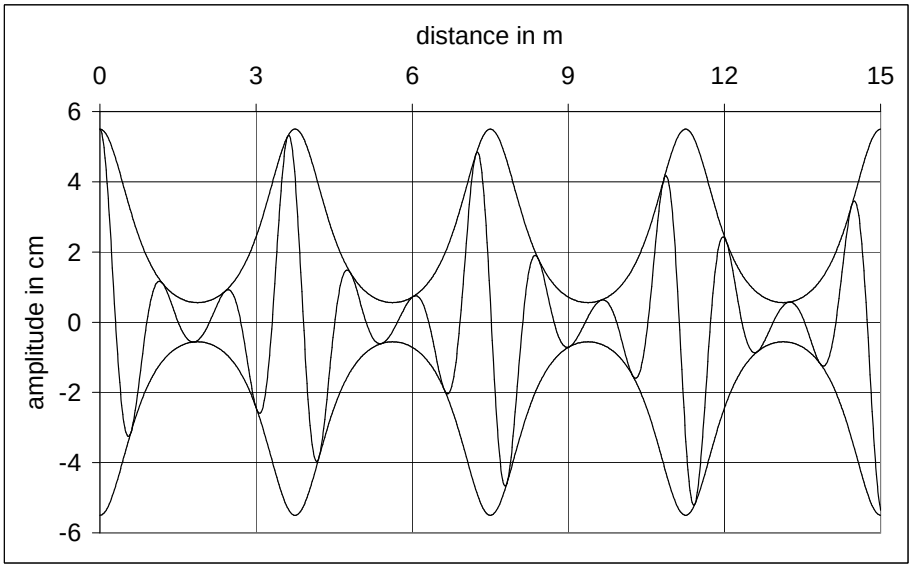

Fig. 21. Envelopes and surface elevation as functions of distance for the perfect periodic soliton solution of the non-linear Schrödinger differential equation

be used only for small distances to explain the behaviour of the waves in our experiments.

It should be noted that in the solution, the parameters are very sensitive. For example, in the iterations a value close to $n_t = 6$ was obtained within the choice of m with four digits. It should be noted that $m = 1$ corresponds to the case the length of the wave group tends to infinity and for groups with six periods in a group in time $m = 0.9887$. A perfect soliton is formed when the non-linear behaviour cancels the influence of dispersion and the solution is stable. This is a very peculiar situation, the parameters are very sensitive and the real behaviour is far from the perfect case when the wave transforms on its path of propagation.

7. Conclusions

1. For all Stokes type waves, regular, with superimposed modifications with small and finite amplitudes the measured frequencies along the flume are very close to the frequencies fixed in the applied time series fed into the control system of the generator. The waves are generated by the oscillations of the piston and the introduced frequencies are preserved along the flume.
2. The measured time series of surface elevations were decomposed by a Kalman filter into two components. The first order component corresponded to the neighbourhood of the dominant frequency and the second order component to its double value. The first order component in a complex number description leads to a simple expression for the envelope as its absolute value.
3. The non-linear Schrödinger differential equation is a useful tool to study the unstable motion of deep water waves when we are mainly interested in amplitudes. The equation is non-linear, but the non-linear term is a simple algebraic one.
4. It's solution essentially corresponds to the first order approximation of a Stokes type wave. Thus in comparisons with experimental data the terms corresponding to the second and third order approximations have to be disregarded.
5. For the Stokes wave the second order term corresponds to the square of the first order term and the third order term to the third power and multiplied by the corresponding coefficients given in the standard formula. A similar formula may be established for Stokes waves with superimposed, small amplitude modifications to estimate the influences.
6. For measured data that look almost like periodic solitons the closed form solution of the non-linear Schrödinger differential equation for a periodic soliton may be used to explain the behaviour in a short space and time interval. This solution is very sensitive to the values of the parameters.

7. The dissipation of energy in the progressing wave along the length of the flume is not negligible. In the presented analysis it was taken into account by introduction of experimental values of amplitudes into the considerations.

References

Benjamin T. B., Feir J. E. (1967), The disintegration of wavetrains on deep waters, Part 1 Theory, *J. Fluid Mech.*, Vol. 27, 417–430.

Lake B. M., Yuen H. C. (1977), A note on some non-linear water wave experiments and the comparison of data with theory, *J. Fluid* Mech., Vol. 83, 75–81.

Lighthill M. J. (1965), Contribution to the theory of waves in non-linear dispersive systems, *J. Inst. Math. Appl.*, Vol. 1, 269–306.

Martin D. U., Yuen H. C., Saffman P. G. (1980), Stability of plane wave solutions of the two-space dimensional non-linear Schrödinger equation, *Wave Motion*, No. 2, 215–229.

Werhausen J. V., Laitone E. V. (1960), Surface Waves, in *Encyclopedia of Physics*, Volume IX, Fluid Dynamics III.

Wilde P., Kozakiewicz A. (1993), Kalman Filter Method in the Analysis of Vibrations Due to Waves, *World Scientific, Advanced Series on Ocean Engineering,* Vol. 6.

Wilde P., Wilde M. (2001), On the generation of water waves in a flume, *Archives of Hydro-Engineering and Environmental Mechanics*, No. 4, 69–83.

Wilde P., Sobierajski E., Chybicki W., Sobczak Ł. (2001), *Theoretical and Experimental Analysis of Stability of Harmonic and Random Wave Trains* (in Polish), Internal Report of the Institute of Hydro-Engineering in Gdańsk, Poland.

Wilde P., Sobierajski E., Chybicki W., Sobczak Ł. (2003), Laboratory investigations of deep-water wave transformation and stability, *Archives of Hydro-Engineering and Environmental Mechanics*, No. 3, 69–83.

Witham G. B. (1974), *Linear and Non-Linear Waves*, Wiley, New York.

Yuen H. C., Lake B. M. (1982), Non-linear dynamics of deep water waves, *Advances in Applied Mechanics*, Vol. 22, 67–229.

Zacharov V. E. (1968), Stability of periodic waves of finite amplitude on the surface of a deep fluid, *Sov. Phys. J. Appl. Mech. Tech. Phys.*, 4, 86–94.